ROYAL SOCIETY
OF CHEMISTRY

www.rsc.org/materialsC

Journal Materials Chemistry C

ARTICLE TYPE

Elastic constants in graphene oxide few-layer films: correlations with interlayer stacking and bonding.

Rafael J. Jiménez Riobóo[a], Esteban Climent-Pascual[a], Xavier Díez-Betriu[a], Félix Jiménez-Villacorta[a], Carlos Prieto[a] and Alicia de Andrés[a]*

We propose a strategy to study the elastic properties of extremely thin graphene oxide (GO) films using Brillouin spectroscopy. The dependence of the surface acoustic wave of a gold capping layer on the structural, chemical and morphological changes occurring to the underneath GO film with temperature is
10 reported and analyzed. At room temperature the shear constant c_{44} is ~17 GPa and hardens up to 28 GPa at 100 ºC due to the partial elimination of embedded water layers and to interlayer distance shrinking. At 200 ºC the almost complete elimination of water induces layer stacking disorder, further GO-GO distance reduction and a significant increase of all elastic constants. The in-plane constants harden due to the partial restoration of sp^2 C network (c_{11}: from 268 to 620 GPa) and the out of plane constants harden due
15 to the H bonds that now directly connect the neighbouring GO layers ($c_{44} \approx 80$ GPa). The obtained Young's moduli are significantly higher than those reported for GO paper because the ultra-thin GO films are highly ordered and there is no macroscopic applied strain during the measurement. The results obtained here are associated to intrinsic properties of GO as in-plane and inter-layer bonding.

Introduction

20 A large spectrum of applications is based on materials derived from graphene oxide monolayers either forming thin films or bulky hybrid materials combined with organic or inorganic compounds where adequate elastic properties are essential. The elastic properties of GO monolayers have been studied by AFM
25 indentation and, for thick GO papers, conventional mechanical techniques were used. The mechanical properties of macroscale GO paper have attracted special interest due to their potential use as reinforced composite components since the elastic properties of graphene were predicted to attain unprecedented values
30 considering its thickness. The elastic properties of free-standing graphene were studied by nanoindentation[1] obtaining a Young's modulus of E =1.0 ± 0.1 TPa, assuming an effective graphene thickness of 0.335 nm. This value is almost identical to that of bulk graphite[2] (1.02 TPa) for the in plane Young's modulus.
35 Brillouin[3] and Raman[4] spectroscopies on multilayer graphene yield also values of different elastic constants very close to graphite.

AFM measurements in GO single layers have delivered effective (when an interlayer distance of 0.7 nm is used) and
40 mean Young's moduli with values of 208± 24 and 250 ± 150 GPa, respectively,[5,6] while the reported measured Young's modulus of thick GO paper are significantly lower and varies over a wide range, 5-42 GPa.[7,8,9,10,11,12] The dispersion within the GO paper values arises from the size- and morphology-dependent

45 effects of testing samples. This macroscale material consists of randomly stacked nano- and micrometer-sized GO flakes that are crumpled, folded, entangled with each other, and interlinked *via* hydrogen bonds among GO's functional groups or through water molecules. Therefore, the load-transfer mechanism between the
50 neighboring GO flakes takes place through GO flakes disentanglement, which is strongly dependent on the particular sample, and through interlayer hydrogen-bonding network.[13,14] Thus, compared to the single layer GO flake, where the measured value is related to the in-plane C network bonding, this
55 macroscale material possesses lower mechanical parameters by one order of magnitude.

Theoretically, simpler microscopic scenarios regarding stoichiometry, size flake, structure (and/or symmetry), morphology and sheet thickness have been used to carry out
60 molecular dynamics (MD) and density functional theory simulations of the stiffness of GO. The calculated Young's modulus of GO sheets covers the range of 290-670 GPa as the density and distribution (random or ordered) of the functional groups and the interlayer distance change.[15,16] It is interesting to
65 note that Young's modulus increases with decreasing degree of functionalization up to ~980 GPa.[17] Also using MD simulations, macroscale GO papers have been theoretically attempted. However, the calculated elastic longitudinal and shear moduli are always lower than the measured effective moduli.[10,11]
70 Peculiarities of the GO paper previously mentioned and the difficulty to perform conventional mechanical experiments on more controlled samples is the reason why, to our knowledge,

there are no reported experimental values for the shear elastic constants of graphene oxide. In the present work we propose a methodology to obtain information on the intrinsic shear elastic constant (related to the interlayer bonding) of graphene oxide through the surface acoustic waves detected by Brillouin spectroscopy of few-layer films of graphene oxide monolayers deposited on glass. The elastic behavior is studied in-situ as a function of the annealing temperature up to 200 ºC across the temperature range, where the embedded water between the graphene oxide layers is expelled out from the film (around 100 ºC), producing the significant shrinking of the interlayer distances. The effect of the elimination of the embedded water molecules and of the partial elimination of the functional groups is analyzed and discussed. Analysis of the results requires insight into different aspects of the film as thickness and density as well as their variation with temperature. These values have been deduced from the reported dependence of the interlayer distances in graphene oxide few-layer films as a function of the temperature obtained from synchrotron radiation diffraction data.[18]

Experimental methods

Samples preparation

The graphene oxide monolayer flakes, GO, were prepared from commercial powder graphite using a modified Hummers method.[19] The GO thin films were obtained by spin coating over glass (microscope slides from "Labbox"). The substrates were cleaned in acetone and water, dipped for 15 min in an aqueous solution of 0.1 M KOH, cleaned with water and dried overnight in an oven at 200ºC. The aqueous suspension of GO was diluted with ethanol to a ratio of ethanol to water of 1:1, in order to favor their hydrophilic behavior. A spreading time from 1 to 3 minutes and a two-step spinning process (300 and 3000 rpm) provide homogeneous films with thickness around 8 nm.[20] Finally, the films were heated at 80ºC for 2 h. A gold film was deposited on top of the graphene oxide/glass sample and simultaneously on a glass substrate, to be used as reference sample, by magnetron sputtering. The reference sample was also used to determine the actual gold thickness. The purpose of this gold film is twofold, one is to protect the graphene oxide film from laser burning since Brillouin experiments on thin films require high power densities and long collecting times. In the present case one hour was a typical collecting time for each spectrum using a power density of 2600 W/cm^2 from an Ar laser (514.5 nm, 150 mW, 120 mm focusing lens). The other purpose is to have a strongly reflecting surface that makes possible obtaining information from the surface acoustic waves (SAW) measured by Brillouin scattering. Two Au/GO/glass samples were studied with Au thickness of ~28 and ~24 nm finding almost identical results.

The GO films thickness was obtained from the Raman intensity of the G peak which was previously calibrated using atomic force microscopy (AFM). A set of 20 points along the film were tested to evaluate the average thickness and dispersion across an area of 5×5 mm^2. The average thickness is 8 ± 2 nm which corresponds to 8 ± 2 graphene oxide monolayers since the interlayer spacing is 1 nm for as deposited samples.
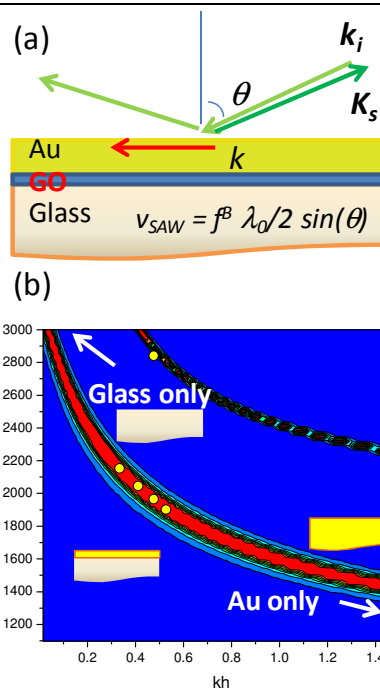

Figure 1 (a) Schema of the experimental configuration where k is the transferred momentum. (b) Measured velocities, yellow dots, and contour plot simulation of $v_{SAW}(kh)$ of the system Au/glass as a function of hk (Au thickness × transferred acoustic wave vector).

Characterization

Atomic Force Microscopy (AFM) measurements were performed in the tapping mode under ambient conditions using a commercial head and software[21] from Nanotec^{TM}. Commercial Nanosensors PPP-NCH-w tips with a spring constant of 34 Nm^{-1} and $f_0 = 270$ kHz were used for topographic characterization.

Surface acoustic waves (SAW) of the Au/GO/glass system and the Au/glass reference sample were studied by measuring the SAW velocity (v_{SAW}) by high resolution Brillouin spectroscopy (HRBS). The experiments were carried out in backscattering geometry with a 2060 Beamlok Spectra Physics Ar-ion single mode laser, 514.5 nm, and a tandem 3+3-Pass Fabry-Pérot interferometer as Brillouin spectrometer.[22] The incoming light is polarized in the scattering plane in order to couple the acoustic wave vector (k) with the surface acoustic wave. In this way, the surface phonon velocity is defined as $v_{SAW} = \omega/k$, where ω is $2\pi f^B$ (f^B is the Brillouin frequency shift), $k = 4\pi(\sin\theta)/\lambda_0$ is the modulus of the involved acoustic wave vector, λ_0 is the laser wavelength in vacuum, and θ is the incident sagittal angle from the normal (see schema in **Figure 1a**). The experiments were performed both at ambient conditions and with the sample heated in a homemade furnace in vacuum (10^{-5} mbar) from room temperature up to 350 ºC.

Simulations

The relevant mechanism giving rise to Brillouin spectra in opaque materials is surface-rippling, unlike transparent materials where the elasto-optic coupling is responsible of Brillouin scattering processes. The numerical simulations of Brillouin

spectra originated from surface acoustic excitations are based on the elastodynamic Green's function method that accounts for the surface ripple mechanism for inelastic scattering of light.[23] Typically, simulations of the SAW velocities (v_{SAW} (kh)) describing an opaque film on top of a substrate, provide its dependence as a function of the adimensional kh magnitude, where k is the modulus of the previously defined acoustic wave vector and h is the film thickness. **Figure 1b** shows the experimental data (yellow dots) and the simulation of v_{SAW} (kh) of the system Au/ glass. By comparing the simulations values with the HRBS experimental data a precise value of the Au film thickness is obtained (23.8 ± 0.4 nm). For small kh values the simulation tends to the substrate (glass) v_{SAW} value ($h = 0$; v_{SAW} = 3183 m/s) and for large kh the simulation tends to the upper film (Au) v_{SAW} value ($kh >> 10$; v_{SAW} = 1142 m/s). The glass substrate density and elastic constants have been measured directly by HRBS in a bare substrate (c_{11} = 85.936 GPa; c_{44} = 30.035 GPa; ρ = 2.488 g/cm^3) and the elastic constants and density of polycrystalline Au have been used for the upper thin film.[24]

Similar calculations as those presented in *Figure 1* are not possible for a three component system as the Au/GO/glass samples. In that case, numerical simulations were done for constant gold thickness and scattering angle (and therefore hk value) and for several values of the GO film thickness. Similar three component numerical simulations have been successfully applied to inorganic systems.[25,26] As in the two component situation the calculations are based on the elastodynamic Green's function method, it is thus necessary to count on reliable values of the densities and elastic constants tensors of the constituting materials (Au, graphene oxide and glass).

Results and discussion

The surface acoustic wave (SAW) of an Au film is modified by the elastic constants of the graphene oxide deposited in between Au film and substrate. Simulations of the SAW velocity of the whole system allow in principle the determination of the shear elastic constants, related to the stacking of the layers, of the sandwiched material. The structural, chemical and morphological changes occurring within the GO few-layer film when annealed will modify the elastic properties of the GO film and therefore variations of the SAW are foreseen.

The strategy to obtain information on the elastic properties of GO few-layer films by Brillouin scattering consists of measuring the changes in the SAW velocity of an Au capping layer induced by a graphene oxide film. Typical HRBS spectra of the Au/glass and Au/GO/glass samples (*Figure 2a*) show narrow peaks around 6.25 and 6.35 GHz, respectively, corresponding to Rayleigh waves. These modes are almost insensitive to surface defects and have a large mean free path that, consequently, provide very narrow peaks useful for precise elastic characterization. Additionally, at higher frequency shifts (around 9 GHz) the Sezawa modes corresponding to the guided modes in the Au film are also discerned and correspond to the upper branch in the simulations of *Figure 1b*. Nevertheless, the low intensity and broad width of these modes do not provide additional information.

The SAW frequency of a film on a substrate depends on the transferred momentum, which is related to the geometry of the experiment (*Figure 1a*) and to its thickness and density. The SAW velocities obtained at several transferred momentums (different incident angles) are found to be systematically larger for the sample with the GO film.
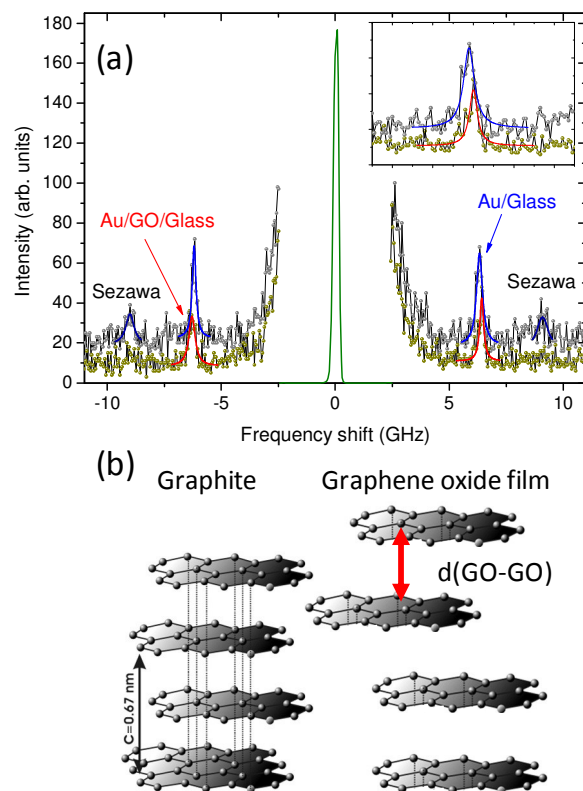

Figure 2 (a) Brillouin spectra at RT of the Au/glass and Au/GO/glass samples showing the surface acoustic wave peaks (Rayleigh and Sezawa) at both sides of the elastically dispersed light. The inset shows a zoom of the SAW peaks with the simulated profiles in continuous lines, red for Au/GO/glass and blue for Au/glass. (b) Schemas of graphite and of a GO film.

The studied system is quite complex and requires combined simulations of the experimental Brillouin scattering data with structural and morphological information. Schemas of graphite and of GO few-layer film are included in *Figure 2b*. The GO flakes lie parallel to the surface mimicking the substrate morphology as the Au layer does. Synchrotron diffraction studies demonstrated that the interlayer distance d(GO-GO) is 1 nm in as-deposited samples and that the stacking is highly regular[18]. In this configuration the weight of the in-plane c_{11} elastic constant in the modification of the SAW velocity is small, being c_{44} the most relevant constant. **Table 1** collects the densities of the GO film for the different temperatures calculated from that of graphite and the measured interlayer distances. The elastic constants of graphite are also included. We have used these densities and the elastic constants of glass and Au collected in Table S1 (Supp. Info.) to perform the calculations of the SAW velocity in the Au(24 nm)/GO(8 nm)/glass sample described later.

The measured SAW velocity at room temperature (1995 m/s at θ

= 55º) is higher than that of the reference sample Au/glass (1966 m/s at θ = 55º), which is, in principle, unexpected considering that the value of c_{44} of graphite (5.05 GPa) is smaller than that of glass (30 GPa) and gold (28.5 GPa).

	Graphite	GO RT	GO 100ºC	GO 200 ºC	B₄C [a]
ρ (g/cm³)	2.2	**0.75**	**0.95**	**1.5**	2.52
d(GO-GO)		**10 Å**	**7.2 Å**	**5 Å**	
c_{11} (GPa)	1060	**268**	**268**	**620**	542.8
c_{33} (GPa)	36.5	**123**	**202**	**578**	534.5
c_{44} (GPa)	5.05	**17 ± 2**	**28 ± 5**	**80 ± 30**	164.8
c_{12} (GPa)	180	**45.5**	**45.5**	**105**	130.6
c_{13} (GPa)	7.9	**27**	**44**	**125**	63.5
c_{66} (GPa)	440	**111.25**	**111.25**	**257.5**	206.2
E_{100} (GPa)	1028.2	**256**	**253**	**582**	507
E_{001} (GPa)	36.4	**118**	**190**	**535**	522

Table 1 Mass density, elastic constants and Young's Moduli of graphite used for the simulations and the results obtained for the GO film (bold characters) at different temperatures. [a] The elastic constants of hexagonal B₄C from[27] are included for comparison.
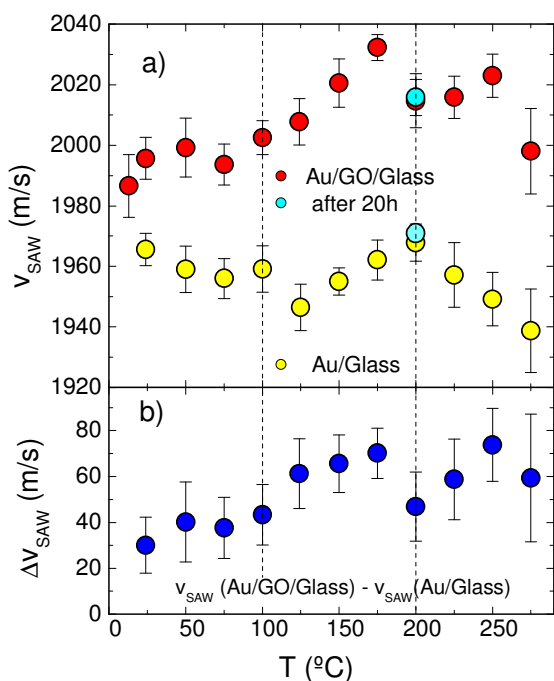

Figure 3 (a) SAW velocities of Au/GO/glass (red circles) and Au/glass reference sample (yellow) as a function of the temperature. The cyan dot corresponds to measures after 20 h. (b) Difference of the velocities in part (a) to evidence the effect of the GO film.

The first approximation to perform the simulations could be using the graphite elastic constants since there are no reported experimental values for the shear constants of GO. Nevertheless the interlayer coupling in GO is quite different from graphite since hydrogen bonds between the water molecules present at the GO-GO interlayer space and the functional groups of graphene oxide, essentially epoxy and hydroxyl groups,[28,29] are expected to

increase substantially the shear elastic constants: O···H bond strengths are typically more than ten times stronger (~320 meV)[29] than interlayer interactions in graphite (~20 meV).[30] Since one water monolayer is reported for interlayer distances around 0.6 – 0.8 nm,[31] two water layers in average can be inferred in the present case (the interlayer distance at RT is 1 nm). Calculations of the bonding energy between the GO layers have shown its dependence on the hydrogen bonds density and type (intra-layer between functional groups or interlayer between functional groups and involving water molecules).[14] Therefore, the c_{44} constant, related to the interaction between the GO layers in GO film, is also expected to vary with the interlayer distance, the number of water layers and the type and density of functional groups. All these parameters change when the film temperature is increased.

In order to study the evolution of the mechanical behavior as the temperature increases, the Brillouin spectra were measured as the Au/glass (yellow dots in *Figure 3a*) and Au/GO/glass samples (red dots) were heated in vacuum up to 325 ºC. Above 250 ºC the quality of the spectra is not adequate probably because modifications occurring in the Au film morphology with temperature (see Supp. Info. Figure S1) while below 250 ºC the results are very stable. The cyan dots in *Figure 3a* correspond to the repeated measurements after 20 h at 200 ºC, showing reproducibility in the measurement and the mechanical stability of the system. The difference of the measured SAW velocities with and without GO film is always above 30 m/s and presents three distinct regions: up to 100 ºC, between 100 ºC and 200 ºC and temperatures above 200 ºC (*Figure 3b*).
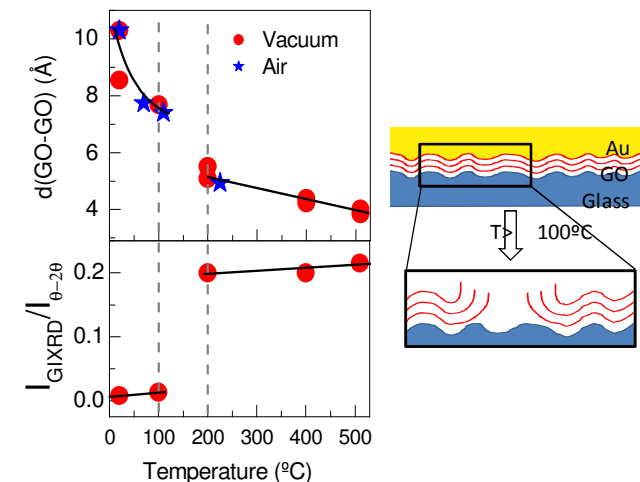

Figure 4 Dependence with temperature of the interlayer distance obtained in θ/2θ scans for GO film in vacuum (red dots) and air (black stars) and of the ratio between the GIXRD and θ/2θ scan intensities. The effect of embedded water ejection on the GO film upon annealing is schematized in the right side.

To understand these results it is necessary to use the information about the temperature dependence of the GO film stacking obtained by Synchrotron X-ray diffraction.[18] The data of *Figure 4* correspond to a GO few-layer film on Si(001). After an initial shrinking of the GO-GO interlayer distance at RT in high vacuum, a monotonous distance decrease occurs from RT to 100ºC. At 200ºC the distance is significantly reduced and the

ratio between the diffracted intensities measured in θ-2θ and grazing incidence (GIXRD) geometries increases drastically. This ratio gives an idea of the fraction of the GO stacks which are not parallel to the surface and how this fraction evolves with temperature. Between 100 and 200 ºC there is a pronounced step in both parameters. This temperature interval coincides with the loss of embedded water allocated in the GO-GO interlayer spacing. The effect of the ejection of water molecules is schematized in the right side of *Figure 4*. Besides the sudden decrease of the interlayer distance, the expelled water produces disorder of the flakes stacking as indicated by the increase of the ratio between the GIXRD and θ/2θ scans (at 200 ºC) since the GIXRD intensity corresponds to orientations of the stacks not parallel to the surface. As the temperature increases, the GO film thickness is reduced and the density increases since the number of GO layers is constant.

SAW Simulations:

The measured interlayer distances at RT, 100 and 200 ºC have been used to estimate the densities of the GO film at the different temperatures, necessary for the simulations. The GO stacked layers are approximated by the hexagonal lattice of graphite with ad-hoc interlayer distances, therefore six elastic constants are required (Table 1). To reduce the number of unknown parameters the following approximations and assumptions have been made:
 i) the c_{11} parameter is chosen from the data in the literature and ii) the elastic constants are split in two sets: those related to c_{11} (c_{11}, c_{12} and c_{66}) and those to c_{44} (c_{44}, c_{33} and c_{13}) which are scaled identically within each set.

These approximations are based on the facts that experimental data on GO only deliver Young's Modulus (E) values and because Graphene oxide films are extremely anisotropic materials where in-plane covalent C-C bonds and inter-plane interactions have very different energy scales. For hexagonal symmetry the Young's modulus in the (a-b) plane is mainly determined by c_{11} and c_{12} elastic constants and the shear elastic constant c_{66} is a linear combination of these two.
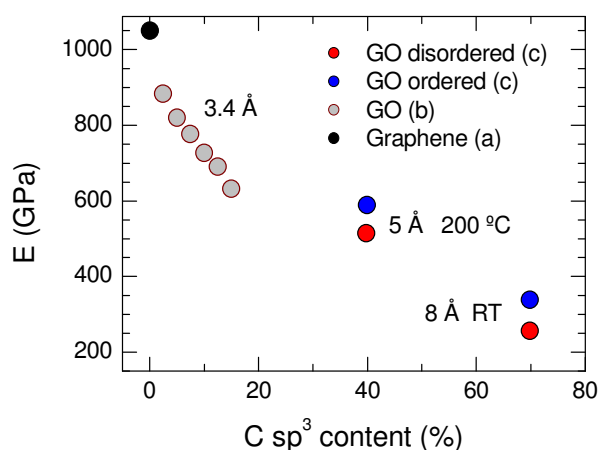

Figure 5 Recalculated Young's modulus values for graphene and different GO from references #1 (a), #17 (b) and #15 (c). The interlayer distances from[18] and sp3 content from[20] have been used.

On the other hand, elastic properties related to interlayer interactions are described by the elastic constants c_{33} and c_{13} and the shear elastic constant c_{44}. Any change in the in-plane and interlayer interactions will be reflected in the related elastic constants and, as a first approximation, identical dependences were assumed for the elastic constants of each set.
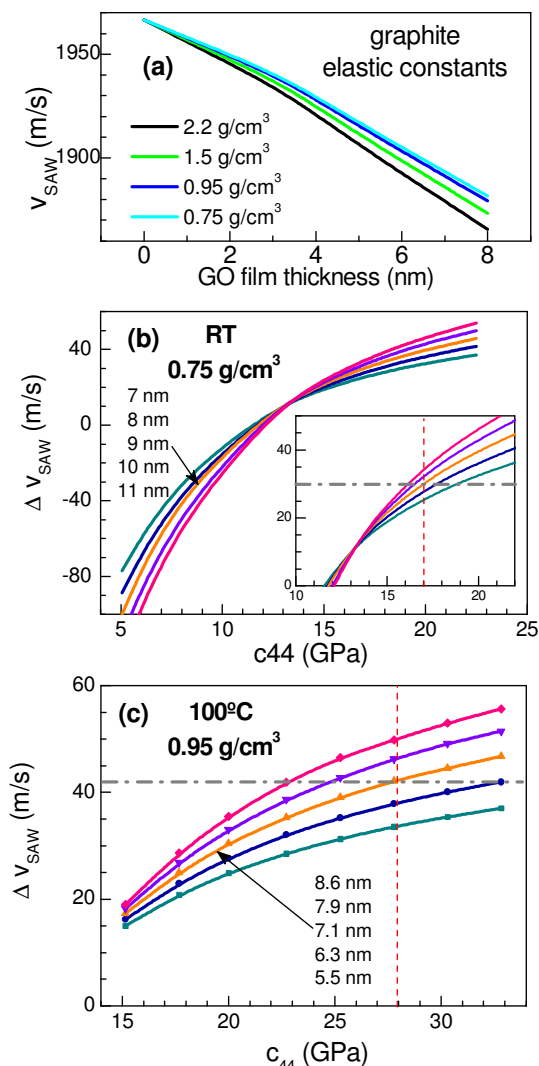

Figure 6 (a) SAW velocity of the system Au/GO/Glass calculated with the graphite elastic constants as a function of the GO thickness for different film densities and $\Delta v_{SAW} = v_{SAW}$ (Au/GO/Glass) - v_{SAW} (Au/Glass) as a function of the c_{44} elastic constant for RT (b) and 100ºC (c) densities. The horizontal dash-dot lines indicate the experimental values.

In *Figure 5*, reported calculated Young's modulus values for graphene and different types of graphene oxides are presented. The collected values have been recalculated using the measured GO-GO distances for samples with the indicated sp3 content. Therefore, for standard GO, with typically around 70% sp3, the calculated Young's modulus is around 250 or 350 GPa for the same fraction of functional groups either disordered or ordered, respectively.[15] The sp3 content of our RT sample is around 70% and therefore we choose E = 256 GPa (the value for disordered

functional groups) which corresponds to c_{11} = 268 GPa, that matches well with the GO monolayer measured values.

It is important to note that, when using the graphite elastic constants, the calculated SAW velocities of the Au/GO/glass system as a function of the GO film thickness (**Figure 6a**) predict their reductions, contrary to the experimentally determined increase. Since c_{11} is smaller in GO than in graphene or graphite it is clear that c_{44} and c_{33} constants have to be higher. Therefore we calculated the SAW velocities as a function of the c_{44} constant (c_{33} and c_{13} are scaled in the same manner) using c_{11} = 268 GPa and the densities for the film at RT and 100ºC (Table 1).

In **Figures 6b and 6c** the differences between the calculated velocities of the Au/GO/glass and Au/glass samples (Δv_{SAW} = v_{SAW} (Au/GO/Glass) - v_{SAW} (Au/Glass)) are presented to be compared with the experimental data of **Figure 2b.** This allows the elimination of the measured small changes in v_{SAW} (Au/Glass) as the temperature increases. The calculations are done for films with different number of GO layers (6, 7, 8, 9 and 10 layers) around the measured average value for the sample (8 monolayers). Since at RT the interlayer distance is 1 nm, the corresponding thickness varies from 7 to 11 nm. As the temperature increases the number of layers is maintained while the thickness is reduced according to the GO-GO distance.

The dependence of Δv_{SAW} as a function of c_{44} is calculated using c_{11}= 268 GPa, c_{12} = 45.5 GPa, c_{66} = 111.25 GPa (c_{33} and c_{13} are changed accordingly to c_{44} values) for the density and film thicknesses corresponding to RT (**Figure 6b**) and 100 ºC (**Figure 6c**). It is interesting to observe, for c_{44} around 13 GPa, a crossing in the dependence of Δv_{SAW} on the thickness. Below this value the thinner film presents the larger v_{SAW} but afterwards the dependence is reversed: the thicker the film the higher the velocity. The horizontal dash-dot lines indicate the experimental measured values which are fitted with c_{44} = 17 ± 2 GPa at RT and 28 ± 5 GPa at 100 ºC. The corresponding values of the other elastic constants are collected in Table 1. The errors in the c_{44} elastic constants are estimated from the experimental error in Δv_{SAW}. The obtained c_{44} values match the range of those deduced from the Young's modulus values measured in GO paper (4 - 40 GPa) and almost coincides with the calculated shear modulus for a GO paper (21 GPa).[13]

As mentioned above, GO paper is a complex and strongly disordered material which consists of randomly stacked GO flakes that are crumpled, folded, entangled with each other, and interlinked *via* a non-uniform network of hydrogen bonds. It is therefore extremely difficult to establish the load-transfer mechanism between neighboring GO flakes. Moreover, the particular characteristics of the folding and entanglement of the GO flakes, probably dependent on the fabrication process of the samples, are relevant for the measured elastic properties and are at the origin of the wide dispersion of reported measured Young's modulus. These extrinsic effects are not important in the present case since the stacking of GO layers in the present ultra-thin films is highly ordered [18] and there is no macroscopic applied strain. Therefore, the results obtained here can be associated with intrinsic effects which are related to the in-plane and inter layer bonding.

The observed increase of c_{44} and c_{33} constants at 100 ºC is due to

changes in the density and configuration of H bonding. At this temperature the measured interlayer GO-GO distance is reduced to 7.2 Å (**Figure 4**) and only one water layer remains between the GO layers strengthening the GO-GO effective bonding as MD calculations have reported.[14]

At 200 ºC elimination of functional groups is already effective and therefore, according to calculations[17] the in-plane c_{11} constant increases because of the reinforcement of the lattice associated to new C=C bonds and rings. The sp^3 fraction at this temperature is around 40 % and the interlayer distance is reduced to 5 Å. The average film thickness is around to 4.5 nm and the density increases to 1.5 g/cm^3. A smaller thickness is less effective in modifying the overall SAW velocity. The observed increase can be due to two effects: one is a further increase of the elastic constants and the other to the changes in the GO layers stacking. At this temperature a fraction of the stacked GO layers, or their edges, have folded up almost perpendicularly to the substrate (**Figure 4**). In this case, the simulations have to include different orientations of the GO stacks and it is necessary to introduce an effective elastic constants matrix for the GO layer. This matrix is formed using the standard Voigt-Reuss-Hill (VRH) average method for different orientations of the c-axis with respect to the normal to the substrate plane[32] (see Supp. Info. for the details of the used matrix and performed average).
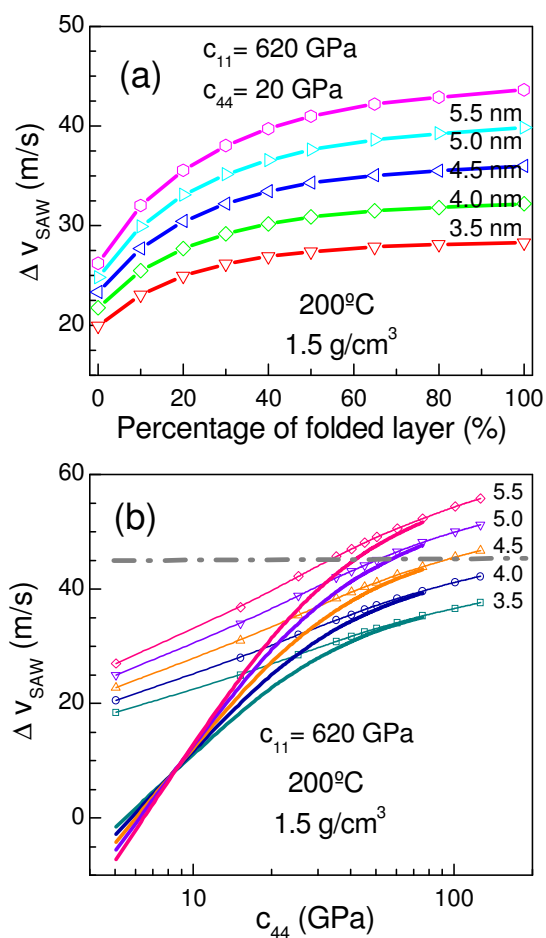

Figure 7 Δv_{SAW}= v_{SAW} (Au/GO/Glass) - v_{SAW} (Au/Glass) for films with thickness from 5.5 to 3.5 nm with an interlayer distance of 5 Å and density of 1.5 g/cm^3 (200ºC) as a function of

(a) the percentage of the folded fraction of the GO layer with c_{11}= 620 GPa and c_{44}= 20 GPa and of (b) the c_{44} constant for 10% folded fraction (continuous lines) and 40% folded fraction (symbols).

The effect of the GO layers folding in the elastic behavior is presented in *Figure 7a* for c_{11}= 620 GPa and c_{44}= 20 GPa. The SAW velocity increases significantly up to about 50 % and much less afterwards. The effect is more important as the film thickness increases being around 100 % increase for the 5.5 nm film.

At 200 ºC the GO-GO distance is further reduced to 5 Å, which favors the formation of H bonds, and the folded fraction increases. In *Figure 7b* the dependence of the velocity is calculated for the density corresponding to 200 ºC considering two different folded fractions (10 % and 40 %). To reach the experimental value, the c_{44} constant has to be increased up to around 80 ± 30 GPa. The large error in the c_{44} value is due on one hand to the experimental error but, at this temperature, it is mainly caused by the small dependence of the SAW velocity with the elastic constants. The simulations indicate that the contribution to the velocity increase due to the folding percentage is very important at low or moderate values of the c_{44} constant but the effect is progressively reduced as c_{44} increases especially for the thinner films. For the average thickness at 200 ºC of our sample, around 3.5 nm, it is not possible to estimate the folded fraction but also it is clear that only an important increase in the elastic constants can explain the high measured velocities. The estimated elastic constants of the GO film at the different temperatures are summarized in Table 1. The elastic constants of another hexagonal compound, B_4C, are included for comparison with the values of the GO film annealed at 200ºC. In both systems c_{11} values are lower than in graphite while c_{44} are significantly higher.

Conclusions

We have shown the effectiveness of the proposed method to obtain information about the elastic properties of extremely thin graphene oxide films by measuring the surface acoustic wave velocity using Brillouin spectroscopy in the Au/GO/substrate system. Intrinsic values of the elastic constants of the GO films are obtained by simulations of the SAW velocity. The dependence of the GO-GO interlayer distance and the GO stacking and orientation on the substrate have been taken into account to evaluate the changes in the elastic constants occurring upon annealing. A hardening of the elastic constants is detected as the temperature increases related to the progressive elimination of the embedded water layers present in the GO film up to 100 ºC. Between 100 ºC and 200 ºC, the violent evaporation of water produces a strong disorder in the layer stacking, which in turn increases significantly the measured SAW velocity. In the as-deposited sample the interlayer distance (1 nm) indicates the presence of two intercalated water layers, their partial elimination leads to interlayer distance shrinking and facilitates the formation of H bonds between the remaining water and the oxygen of OH and epoxide groups, which are responsible for the increase of the c_{44} and related constants up to around 100 ºC. As the temperature further increases, water is almost completely eliminated, the GO-GO distance is further decreased and the functional groups,

mainly epoxide and OH groups, begin to be removed increasing the c_{11} constant from 260 GPa (at RT) to around 620 GPa. H bridges can be then established connecting OH and epoxide groups of two nearest GO layers which increase the shear elastic constants, in particular c_{44} increases from 17 GPa at RT to around 80 GPa. The out of plane elastic constants and Young's modulus in the [001] direction are significantly higher in GO few-layer films than those reported for graphene multilayers because of the different nature of the interlayer bonding. The elastic properties are demonstrated to be strongly sensitive to water content and to GO-GO distance.

Acknowledgments

Notes and references

ᵃ Instituto de Ciencia de Materiales de Madrid, Consejo Superior de Investigaciones Científicas. Cantoblanco 28049 Madrid, Spain.
* E-mail: ada@icmm.csic.es

Electronic Supplementary Information (ESI) available: AFM images and roughness analysis of the Au/glass and Au/GO/glass samples (Figure S1), elastic constants and mass densities of gold and glass used for the calculations (Table S1) and details on the simulations and calculations of the Young's modulus. See DOI: 10.1039/b000000x/

References

1   Lee, C.; Wei, X.; Kysar, J. W.; Hone, J. Measurement of the elastic properties and intrinsic strength of monolayer graphene. *Science (New York, N.Y.)* **2008**, *321*, 385–8.
2   Blakslee, O.; Proctor, D.; E. J. Seldin, G. B. Spence, T. W. Elastic Constants of Compression-annealed Pyrolytic Graphite. *Journal of Applied Physics* **1970**, *41*, 3373–3382.
3   Z.K. Wang, H.S. Lim, S.C. Ng, B. Özyilmaz, M.H. Kuok, Carbon, 46, 2133-2136 (2008)
4   Tan, P. H.; Han, W. P.; Zhao, W. J.; Wu, Z. H.; Chang, K.; Wang, H.; Wang, Y. F.; Bonini, N.; Marzari, N.; Pugno, N.; Savini, G.; Lombardo, a; Ferrari, a C. *Nature materials* **2012**, *11*, 294–300. The shear mode of multilayer graphene.
5   Gómez-Navarro, C.; Burghard, M.; Kern, K. Elastic Properties of Chemically Derived Single Graphene Sheets. Nano Lett. 2008, 8, 2045–2049.
    6 Suk, J. W.; Piner, R. D.; An, J.; Ruoff, R. S. Mechanical Properties of Monolayer Graphene Oxide. *ACS Nano* **2010**, *4*, 6557–6564.
7   Dikin, D. A; Stankovich, S.; Zimney, E. J.; Piner, R. D.; Dommett, G. H. B.; Evmenenko, G.; Nguyen, S. T.; Ruoff, R. S. Preparation and Characterization of Graphene Oxide Paper. Nature 2007, 448, 457–460
8   Zhu, Y.; Park, S.; Lee, K.-S.; Bozoklu, G.; Cai, W.; Nguyen, S. T.; Ruoff, R. S. Graphene Oxide Papers Modified by Divalent Ions—

Enhancing Mechanical Properties via Chemical Cross-Linking. ACS Appl. Mater. Interfaces 2008, 2, 572–578

9   Murali, S.; Cai, W.; Li, X.; Suk, J. W.; Potts, J. R.; Ruoff, R. S. Graphene and Graphene Oxide: Synthesis, Properties, and Applications. Adv. Mater. 2010, 22, 3906–3924

10   Compton, O. C.; Nguyen, S. T. Graphene Oxide, Highly Reduced Graphene Oxide, and Graphene: Versatile Building Blocks for Carbon-Based Materials. Small 2010, 6, 711–723

11   Gao, Y.; Liu, L.-Q.; Zu, S.-Z.; Peng, K.; Zhou, D.; Han, B.-H.; Zhang, Z. The Effect of Interlayer Adhesion on the Mechanical Behaviors of Macroscopic Graphene Oxide Papers. *ACS Nano* **2011**, *5*, 2134–2141.

12   Cheng, Q.; Wu, M.; Li, M.; Jiang, L.; Tang, Z. Ultratough Artificial Nacre Based on Conjugated Cross-Linked Graphene Oxide. Angew. Chemie 2013, 125, 3838–3843

13 Compton, O. C.; Cranford, S. W.; Putz, K. W.; An, Z.; Brinson, L. C.; Buehler, M. J.; Nguyen, S. T. Tuning the Mechanical Properties of Graphene Oxide Paper and Its Associated Polymer Nanocomposites by Controlling Cooperative Intersheet Hydrogen Bonding. ACS Nano 2012, 6, 2008–20191

14   Medhekar, N. V; Ramasubramaniam, A.; Ruoff, R. S.; Shenoy, V. B. Hydrogen Bond Networks in Graphene Oxide Composite Paper: Structure and Mechanical Properties. ACS Nano 2010, 4, 2300–2306

15   Liu, L.; Zhang, J.; Zhao, J.; Liu, F. Mechanical Properties of Graphene Oxides. *Nanoscale* **2012**, *4*, 5910–5916.

16   Peng, Q.; Ji, W.; De, S. Mechanical Properties of Graphyne Monolayers: A First-Principles Study. *Phys. Chem. Chem. Phys.* **2012**, *14*, 13385–13391.

17   Zheng, Q.; Geng, Y.; Wang, S.; Li, Z.; Kim, J.-K. Effects of Functional Groups on the Mechanical and Wrinkling Properties of Graphene Sheets. *Carbon N. Y.* **2010**, *48*, 4315–4322.

18   Díez-Betriu, X.; Mompeán, F. J.; Munuera, C.; Rubio-Zuazo, J.; Menéndez, R.; Castro, G. R.; de Andrés, A. Graphene-oxide stacking and defects in few-layer films: Impact of thermal and chemical reduction. *Carbon* **2014,** 80**,** 40-49.

19   Botas, C.; Álvarez, P.; Blanco, C.; Gutierrez,M.D.; Ares, P.; Zamani, R. *et al.* Tailored graphene materials by chemical reduction of graphene oxides of different atomic structure *RSC Advances* **2012**; 2; 9643-9650.

20   Díez-Betriu X., Álvarez S., Botas C., Álvarez P., Sánchez-Marcos J., Prieto C. *et al.* Raman spectroscopy for the study of reduction mechanisms and optimization of conductivity in graphene oxide thin films *J. Mater. Chem. C* **2013**; 1; 6905.

21   Horcas I, Fernández R, Gómez-Rodríguez J M, Colchero J, Gómez-Herrero J and Baró A M 2007 *Rev. Sci. Instrum.* **78** 013705

22   Sandercock J. R. Light Scattering in Solids III, Applied Physics Vol. 51, edited by M. Cardona and G. Güntherodt (Springer-Verlag, Berlin, 1989)

23   Zhang, X.; Comins, J.; Every, A.; Stoddart, P. Surface Brillouin Scattering Study of the Surface Excitations in Amorphous Silicon Layers Produced by Ion Bombardment. *Phys Rev B* **1998**, *58*, 677–685.

24   E. Salas, R. J. Jiménez Riobóo, C. Prieto, and A. G. Every, Surface acoustic wave velocity of gold films deposited on silicon substrates at different temperatures, J. Appl. Phys. 110, 023503 (2011).

25   R. J. Jiménez Riobóo, E. Rodríguez-Cañas, M. Vila, C. Prieto, F. Calle, T. Palacios, M.A. Sánchez, F. Omnès, O. Ambacher, B. Assouar, O. Elmazria, Hypersonic characterization of sound propagation velocity in AlxGa1-xN thin films, *Journal of Applied Physics,* **2002**, 92, 6868-6874.

26   E. Céspedes, R. J. Jiménez Riobóo, M. Vila and C. Prieto, Brillouin Light Scattering Characterization of the Surface Acoustic Waves Velocity in ZnO/Si3N4/Si(100) System, *Superlattices and Microstructures*, **2006**, 39, 75-82.

27   McClellan K.J., Chu F., Roper J.M. and Shindo I., J. Mater. Sci., **2001**, *36*, 3403

28   Dreyer, D. R.; Park, S.; Bielawski, C. W.; Ruoff, R. S. The Chemistry of Graphene Oxide. *Chem. Soc. Rev.* **2010**, *39*, 228–240

29   Medhekar, N. V; Ramasubramaniam, A.; Ruoff, R. S.; Shenoy, V. B. Hydrogen Bond Networks in Graphene Oxide Composite Paper: Structure and Mechanical Properties. *ACS Nano* **2010**, *4*, 2300–2306

30   Charlier, J.; Gonze, X.; Michenaud, J. *EPL (Europhysics Letters)* **1994**, *28*, 403–408. Graphite interplanar bonding: electronic delocalization and van der Waals interaction.

31   Buchsteiner, A.; Lerf, A.; Pieper, J. Water Dynamics in Graphite Oxide Investigated with Neutron Scattering. *The Journal of Physical Chemistry B* **2006**, *110*, 22328–22338.

32   Grimvall G. Thermophysical Properties of Materials, edited by E. P. Wohlfarth (North-Holland, Amsterdam, 1986)

Graphical abstract

The dependence of the elastic constants of graphene oxide films with temperature is obtained and analysed in terms of in-plane and interlayer bonding.